Effects of potassium doping on the composition, structure and carbon dioxide chemisorption of Na_2ZrO_3

A. Sandoval-Díaz and H. Pfeiffer*
Instituto de Investigaciones en Materiales, Universidad Nacional Autónoma de México,
Circuito exterior s/n, Ciudad Universitaria, Del. Coyoacán, 04510, México D.F., Mexico.

Recibido el 26 de octubre de 2007; aceptado el 15 de enero de 2008

Solid solutions of sodium and potassium metazirconate, $Na_{2-x}K_xZrO_3$, were prepared by coprecipitation. Then, samples were characterized by powder X-ray diffraction, scanning electron microscopy and thermogravimetric analysis. Results show that the solubility limits of potassium in Na_2ZrO_3 is 0.2, $Na_{1.8}K_{0.2}ZrO_3$, and the addition of potassium produced the formation of needle-like particles. Furthermore, $Na_{2-x}K_xZrO_3$ solid solutions were tested as CO_2 captors. The analyses of these materials showed that, although all the solid solutions present similar behaviors, the chemisorption and diffusion kinetics were enhanced by the addition of potassium. $Na_{1.6}K_{0.4}ZrO_3$ seems to be the best solid solution for the CO_2 capture. The differences observed in the CO_2 sorption processes were explained by the different ionic radii of sodium and potassium and with thermodynamic data.

Keywords: Absorption; carbon dioxide; sodium and potassium zirconate.

Soluciones sólidas de zirconato de sodio y potasio, $Na_{2-x}K_xZrO_3$, fueron preparados por el método de coprecipitación. La caracterización de estos materiales fue realizada por difracción de rayos X, microscopia electrónica de barrido y análisis termogravimétrico. Los resultados muestran que el límite de solubilidad de potasio en el zirconato de sodio es 0.2, $Na_{1.8}K_{0.2}ZrO_3$. Además, la adición de potasio indujo una morfología, en las partículas del cerámico, en forma de agujas. Posteriormente, las diferentes soluciones sólidas fueron probadas para la captura de CO_2. Aparentemente, $Na_{1.6}K_{0.4}ZrO_3$ resultó ser el mejor cerámico para la captura de CO_2. Los diferentes análisis mostraron que, a pesar de que el comportamiento fue parecido para todas las muestras, los procesos de quimisorción y difusión se incrementaron con la adición de potasio. Los resultados fueron explicados en función de los radios iónicos de sodio y potasio, así como con factores termodinámicos.

Descriptores: Absorción; dióxido de carbono; zirconato de sodio y potasio.

PACS: 61.05.cp; 61.66; 68.37.Hk; 68.43.-h

1. Introduction

In the last century, the use of oil and many other carbon resources have dramatically increased the production of CO_2. As a consequence, the earth has been increasing its temperature through the so-called “green house effect” [1-2]. Therefore, CO_2 emissions need to be reduced or at least controlled in different ways [3-5].

In order to trap CO_2 from the environment, some studies have focused on its chemisorption process. In this way, alkaline and earth-alkaline ceramics seem to be a good option. For example, Li_2O presents excellent kinetic and thermodynamic properties such as being CO_2 absorbent [6]. Other alkaline and earth-alkaline oxides and hydroxides, such as LiOH, NaOH, BaO, MgO and CaO, show similar behaviors [7-10]. However, most of these materials present a problem: they increase their volume by up to 250% during the CO_2 chemisorption. Therefore, attempting to solve this issue, Nakagawa and Ohashi tested lithium zirconate (Li_2ZrO_3) for the same objective [11]. They found that, although Li_2ZrO_3 presents similar chemisorption properties, this material did not vary its volume so much. Moreover, it was found that potassium increases the kinetic reaction, due to its low fusion temperature [12-13]. Since the publication of these papers, several works have reported the CO_2 chemisorption on different lithium, sodium and potassium zirconates, silicates and titanates, among others [6, 14-17]. Therefore, the aim of this work was to analyze systematically the K-doping of Na_2ZrO_3 $(Na_{2-x}K_xZrO_3)$, and its implications during the kinetic sorption of CO_2.

2. Experimental section

The co-precipitation method was used to obtain sodium-potassium zirconates. Stoichiometric amounts of sodium carbonate (Na_2CO_3, Aldrich), potassium carbonate (K_2CO_3, Aldrich) and zirconium acetate ($Zr(OCH_3)_4$, Aldrich) were dissolved and mixed. Each solution was stirred in water for 1 hour and then heat-treated at 70^{o}C, until the precipitate dried. Finally, the powders were pulverized and calcined at 900^{o}C for 4 hours. The Na:K molar ratio was varied from 0 to 1.0 to obtain the solid solutions, $Na_{2-x}K_xZrO_3$. These nominal values were used to label the samples, *i.e.* $Na_{1.8}K_{0.2}ZrO_3$.

Samples were characterized by X-ray diffraction (XRD), scanning electron microscopy (SEM) and thermogravimetric analysis (TGA). To obtain the X-ray diffraction patterns, a BRUKER axs (model D8 Advance) diffractometer was used. The various compounds were identified by the corresponding JCPDS files (Joint Committee on Powder Diffraction Standards), and their percentages were estimated from the total area under the most intense diffraction peak for each phase. A scanning electron microscope (SEM), Stereoscan 440 Cambridge, was used to determine the morphology of the samples. As these materials are non-conductive, powders were covered with gold. CO_2 sorption analyses were performed in a 2950 Thermogravimetric Analyzer, TA Instruments. Samples were heat treated with a heating rate of 5°C min^{-1} from room temperature to 1000°C, into a CO_2 flux. Finally, isothermal experiments were performed in the same equipment at 550°C under a flux of CO_2.

3. Results and discussion

Samples of Na_2ZrO_3 alone or doped with potassium, $Na_{2-x}K_xZrO_3$, were obtained using different Na:K molar ratios. These diffractograms are shown in Figure 1. Samples with x= 0 and 0.2 only showed the presence of Na_2ZrO_3. However, if the $x$value was increased to 0.4, a different phase was also found. In this case, ZrO_2 was detected. Finally, if the Na:K molar ratio was increased to 1:1, the quantities of ZrO_2 increased as well.

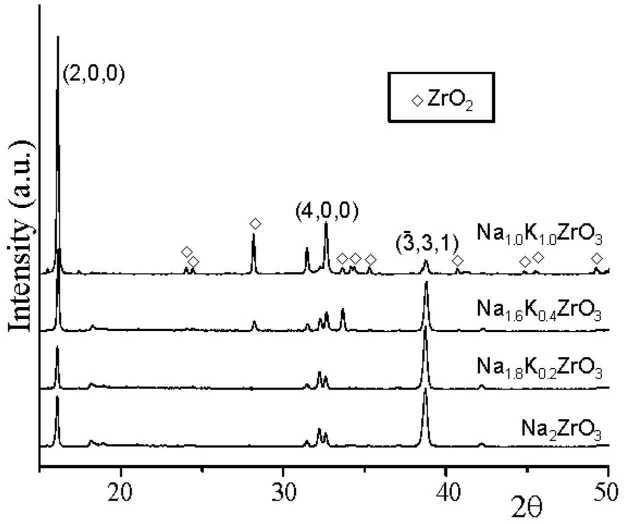

FIGURE 1. XRD patterns of the Na_2ZrO_3 and different $Na_{2-x}K_xZrO_3$ solid solutions.

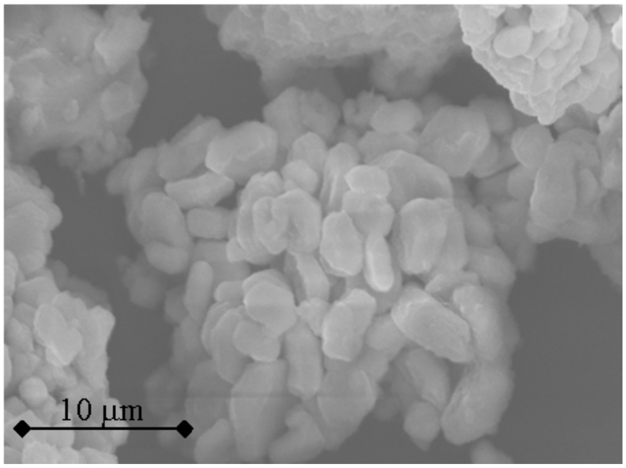

FIGURE 2. SEM image of the Na_2ZrO_3 powders.

The presence of ZrO_2 and the non-identification of any potassium phase strongly suggest that potassium is being lost in some way. It has been reported that potassium zirconates are not very stable; all of them decompose at lower temperatures than 750°C. In these compounds, most of the potassium atoms sublime and the others remain as dopant into the zirconium oxide [12,18]. Perhaps for the samples prepared at 900°C, most of the potassium should sublime. The results indicate that the solubility limit of potassium in Na_2ZrO_3 is equal to 0.2, producing the following nominal formula: $Na_{1.8}K_{0.2}ZrO_3$. However, it cannot be conclusive, due to the high tendency of potassium to sublime.

Something else comes out of observing the XRD patterns: the (2,0,0) and (4,0,0) peaks of the Na_2ZrO_3 phase significantly increased their intensities as a function of the potassium content, in comparison to the (-3,3,1) peak, which is labeled as the 100% peak intensity in the JCPDS files. Therefore, there is a preferential orientation produced by the addition of potassium on the [2,0,0] family peaks. This effect may be produced during the potassium sublimation, or because the potassium atoms are mainly located over this family of planes.

Scanning electron images of Na_2ZrO_3 and $NaKZrO_3$ are shown in Figs. 2 and 3, respectively. In the first case, the Na_2ZrO_3 has a homogeneous polyhedral shape, with a particle size of 3 μm (Fig. 2).

In addition, these particles seem to be agglomerated, forming large agglomerates of up to 30-40 μm. On the other hand, the addition of potassium modified the morphology of the samples. Figure 3, which is a backscattered electron image, shows the presence of two different phases. This result agrees with the XRD results, where ZrO_2 had already been detected. In this case, the lighter phase corresponds to ZrO_2 ($\bar{Z} = 19.66$) and the dark phase is the sodium zirconate ($\bar{Z} = 14.3$). ZrO_2 presents a polygonal shape with a particle size of 4 μm, on average. These particles seem to be immersed in the dark phase, Na_2ZrO_3, which has a needle-like shape. The needle-like morphology, observed in this sample, is in agreement with the preferential orientation observed by XRD.

Na_2ZrO_3, is a good CO_2 absorbent material. So, if the $Na_{2-x}K_xZrO_3$ solid solutions present a synergetic effect, they should capture more CO_2, through the following reaction:

$$Na_{2-x}K_xZrO_3 + CO_2 \rightarrow (Na_{2-x}K_x)CO_3 + ZrO_2 \quad (1)$$

where, $(Na_{2-x}K_x)CO_3$ represents, merely, a mixture of K_2CO_3 and Na_2CO_3.

The different samples analyzed by TGA presented CO_2 absorption (Fig. 4). First, Na_2ZrO_3 increased its weight in two different steps: first there is just a superficial absorption between 100 and 350°C; then, at higher temperatures (400-800°C), the chemisorption is completed. This result is in total agreement with previous reports [16]. The $Na_{1.6}K_{0.4}ZrO_3$ sample presented a very similar trend, but this sample absorbed 2 wt% more CO_2. It seems that the addition of potassium does enhance the CO_2 absorption. Conversely, $NaKZrO_3$ presented some differences. At lower temperatures than 100°C, the sample lost 1 wt%, which must corresponds to the dehydration of the sample. This effect was not observed for the other samples. Hence, the sample became more hygroscopic with the addition of potassium. Perhaps, the residual potassium is adsorbing water. The second difference is in the shape of the absorption process. In this case, the superficial absorption cannot be distinguished from the bulk absorption. Therefore, the kinetic of the absorption process may be changed by the addition of potassium. Finally, this sample captures less CO_2, in comparison to the previous samples. However, it must be pointed out that this sample contains ZrO_2, which does not absorb CO_2.

In order to analyze wheter the kinetic reaction is modified due to the potassium doping, the different samples were isothermically analyzed. Figure 5 shows the isothermal graphs at 550°C. When the Na_2ZrO_3 curve was compared to $Li_{1.6}Na_{0.4}ZrO_3$ and $NaKZrO_3$ samples, Na_2ZrO_3 absorbed 13.3 wt%, after 300 min, whereas $Na_{1.6}K_{0.4}ZrO_3$ and $NaKZrO_3$ increased the absorption to 14.7 wt% and 14.1 wt%, respectively, in the same period of time. It must be pointed out that the CO_2 absorption quantities obtained for $NaKZrO_3$ were adjusted as a function of the ceramic content (see XRD analysis). Although the CO_2 sorption in Na_2ZrO_3 was not much lower than those in the samples containing potassium, it was obvious that at short times (between 0 and 50 min), the kinetic is significantly improved by the presence of potassium, as shown by the slope of the curves, 2.14, 2.16 and 2.22 wt% min^{-1} for Na_2ZrO_3, $Na_{1.6}K_{0.4}ZrO_3$ and $NaKZrO_3$, respectively. Hence, potassium atoms must locally modify the structure of Na_2ZrO_3. As potassium atoms are larger than sodium atoms, the Na_2ZrO_3 structure was probably expanded, favoring an easier diffusion of the sodium atoms to reach the CO_2 molecules. Another explanation can be related to the preferential orientation observed by XRD and SEM, which may allow a higher surface area, and therefore, a higher possibility of reaction between the ceramic and the CO_2. Finally, another option proposed in the literature indicates that potassium becomes liquid and works as a transport for the atom diffusion.

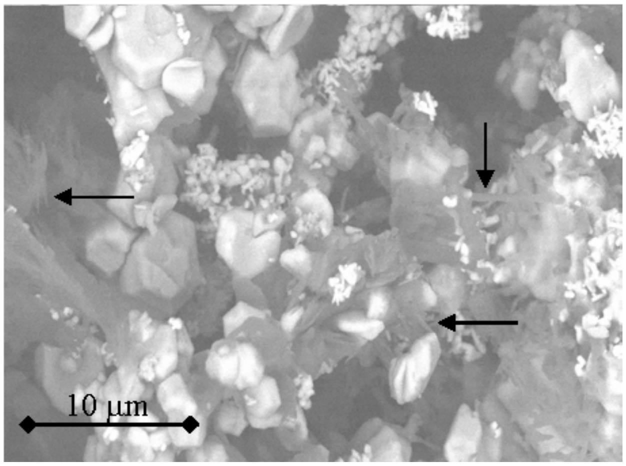

FIGURE 3. Backscattered electron image of the $NaKZrO_3$ powders. Light particles correspond to ZrO_2 and dark particles to Na_2ZrO_3. The arrows indicate the needle-like formation.

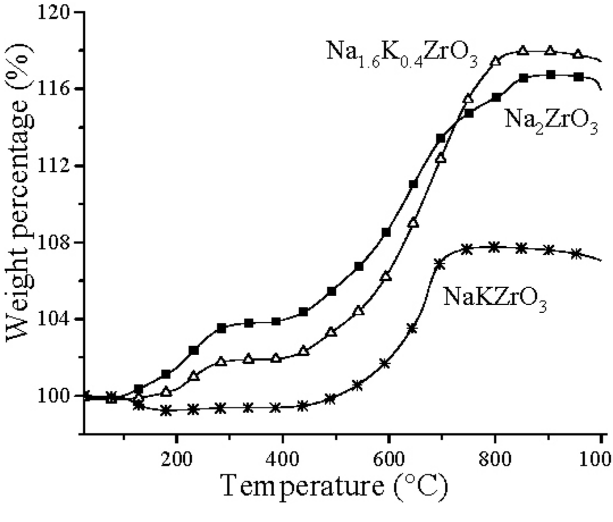

FIGURE 4. Thermogravimetric analyses of different $Na_{2-x}K_xZrO_3$ solid solutions in a flux of CO_2.

TABLE I. Parameters obtained from the experimental data fitted to a double exponential model.

Sample	k_1 (seg^{-1})	k_2 (seg^{-1})
Na_2ZrO_3	0.00203	0.00012
$Na_{1.6}K_{0.4}ZrO_3$	0.00221	0.00013
$NaKZrO_3$	0.00544	0.00031

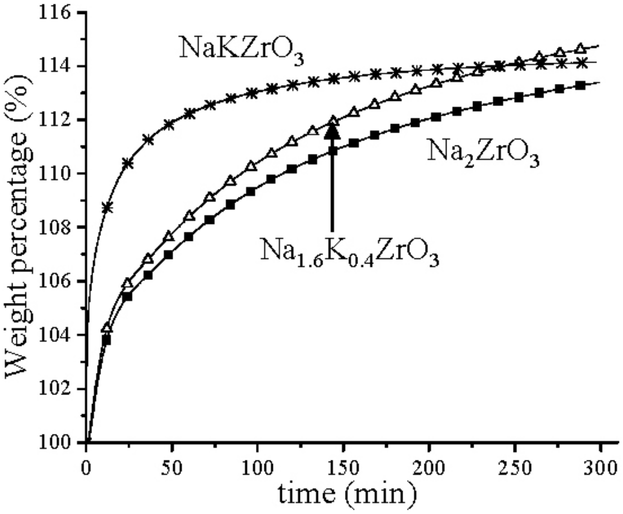

FIGURE 5. Isothermal analyses of $Na_{2-x}K_xZrO_3$ solid solutions heat treated at 550°C in a flux of CO_2. The symbols correspond to the data, and the lines to the model fitted.

The same Fig. 5 shows that all the isotherms fitted into a double exponential model [Eq. (2)]:

$$y = A\exp^{-k_1 t} + B\exp^{-k_2 t} + C \tag{2}$$

where y represents the weight percentage of CO_2 absorbed, t is the time, k_1 andk_2 are the exponential constants and A, B and C are the pre-exponential factors. The values obtained for each sample are presented Table I. This adjustment is in total agreement with previous reports, which propose that these kinds of ceramics absorb CO_2 through two different processes; at the beginning, CO_2 reacts with the surface of the ceramic, producing the alkaline carbonate. Later, once the carbonate external layer is created, the diffusion of the alkaline element begins, through the carbonate layer, to react with the CO_2 at the surface of the particles [6,19]. Here, Na_2ZrO_3 reacts with CO_2, producing an external layer of Na_2CO_3. Then, sodium and potassium have to diffuse through the carbonate layer to be able to react with the CO_2. As can be seen in Table I, k_1 (chemisorption process) is one order of magnitude larger than k_2 (diffusion process). Therefore, kinetically, the limiting step of the whole process is the diffusion. In addition, the k_1 andk_2 values increased with the addition of potassium.

This confirms that potassium enhances the CO_2 absorption in both the superficial reaction and the bulk diffusion processes.

Finally, as the formation enthalpy (ΔH_f) of sodium and potassium carbonates are very similar, -1130.7 kJ/mol and -1151 kJ/mol, respectively [20], the improvement of the CO_2 absorption must only be associated with kinetic factors. In other words, as the energy required for the formation of both carbonates is practically the same, the improvement observed in the CO_2 capture cannot be explained on thermodynamic bases. Therefore, only kinetic factors should be considered.

4. Conclusions

$Na_{2-x}K_xZrO_3$ solid solutions were prepared by precipitation. The limits of potassium solubility to Na_2ZrO_3 were determined by XRD, and it was x = 0.2. In addition, during the characterization of these solid solutions, the formation of a specific morphology was detected by SEM; the ceramics acquired a needle-like shape.

$Na_{2-x}K_xZrO_3$ solid solutions presented a high CO_2 absorption capacity. It was proved that the addition of potassium increased the kinetic of chemisorption and diffusion, according to the model adjusted to the isothermal results. The results were explained in terms of the ionic radius of potassium and sodium, as well as in thermodynamic terms. According to these results, $Na_{1.6}K_{0.4}ZrO_3$ seems to be the best solid solution for the CO_2 capture, because higher potassium concentrations produce high quantities of ZrO_2, which is not able to absorb CO_2, decreasing the efficiency of the ceramic.

Acknowledgements

This work was financially supported by the Mexican government through CONACYT by the projects 23418-SEMARNAT-CONACYT and 46522Q-SEP-CONACYT. Sandoval-Díaz A. wishes to thank CONACYT for its financial support (46522Q-SEP-CONACYT). Furthermore, the authors wished to thank L. Baños and E. Fregoso for technical help in the XRD and thermal analyses, respectively.

[∗] Corresponding Author. Phone: +52(55)56224627, Fax: +52 (55)56161371, e-mail: pfeiffer@iim.unam.mx

1. X. Wei, X. Liu and M. Deeba, *Appl. Catal. B: Environ.* **58** (2005) 41.
2. M.S. Kwak, J. Hwang, C.O. Park, N. Miura, and N. Yamazoe, *Sens. Act. B* **56** (1999) 59.
3. E. Ocho-Fernández, M. Rønning, T. Grande, and D. Chen, *Chem. Mater.* **18** (2006) 1383.
4. A. Macario, A. Katovic, G. Giordano, F. Iucolano, and D. Caputo, *Microporous Mesoporous Mater*. **81** (2005) 139.
5. K. Nomura, K. Tokumistu, T. Hayakawa, and Z. Homonnay, *J. Radioanal. Nucl. Chem*. **246** (2000) 69.
6. H. Mosqueda, C. Vazquez, P. Bosch, and H. Pfeiffer, *Chem. Mater.* **18** (2006) 2307.
7. E.J. Karlsen, M.A. Nygren, and L.G.M. Pettersson, *J. Phys. Chem. B* **107** (2003) 7795.
8. M. Tutuianu, O.R. Inderwildi, W.G. Bessler, and J. Warnatz, *J. Phys. Chem. B* **110** (2006) 17484.
9. J.C. Abanades, G. Grasa, M. Alonso, N. Rodriguez, E.J. Anthony, and L.M. Romeo, *Environ. Sci. Technol*. **41** (2007) 5523.
10. M. Chen, N. Wang, J. Yu, and A. Yamaguchi, *J. Europ. Ceram Soc.* **27** (2007) 1953.
11. K. Nakagawa and T. Ohashi, *J. Electrochem. Soc.* **145** (1998) 1344.
12. M.Y. Veliz-Enriquez, G. Gonzalez, and H. Pfeiffer, *J. Solid State Chem.* **180** (2007) 2485.
13. J.I. Ida, R. Xiong, and Y.S. Lin, *Sep. Purif. Technol*. **36** (2004) 41.
14. H. Pfeiffer and P. Bosch, *Chem. Mater.* **17** (2005) 1704.
15. H. Pfeiffer, E. Lima, and P. Bosch, *Chem. Mater.* **18** (2006) 2642.
16. H. Pfeiffer, C. Vazquez, V.H. Lara and P. Bosch, *Chem. Mater.* **19** (2007) 922.
17. M.J. Venegas, E. Fregoso-Israel, R. Escamilla, and H. Pfeiffer, *Ind. Eng. Chem. Res.* **46** (2007) 2407.
18. S. Dash, D.D. Sood, and R. Prasad, *J. Nucl. Mater.* **228** (1996) 83.
19. R. Xiong, J. Ida, and Y.S. Lin, *Chem. Eng. Scien.* **58** (2003) 4377.
20. R.D. Lide, *CRC Handbook of Chemistry and Physics* 73^{RD} Edition (CRC Press, Inc., 1992-1993).